Antiviral Research 81 (2009) 47–55

Contents lists available at ScienceDirect

Antiviral Research

journal homepage: www.elsevier.com/locate/antiviral

Non-nucleoside HIV-1 reverse transcriptase inhibitors *di-halo*-indolyl aryl sulfones achieve tight binding to drug-resistant mutants by targeting the enzyme–substrate complex

Alberta Samuele[a], Alexandra Kataropoulou[a], Marco Viola[a], Samantha Zanoli[a], Giuseppe La Regina[b], Francesco Piscitelli[b], Romano Silvestri[b,*], Giovanni Maga[a,**]

[a] *Department of DNA Enzymology and Molecular Virology, Institute of Molecular Genetics, National Research Council, IGM-CNR, via Abbiategrasso 207, 27100 Pavia, Italy*
[b] *Pasteur Institute, Cenci-Bolognetti Foundation, Department of Pharmaceutical Studies, Sapienza of Rome, P.le Aldo Moro 5, I-00185 Rome, Italy*

ARTICLE INFO

Article history:
Received 23 June 2008
Received in revised form 7 August 2008
Accepted 9 September 2008

Keywords:
HIV-1
NNRTIs
Drug resistance
Enzyme kinetics
AIDS

ABSTRACT

Indolyl aryl sulfone (IAS) non-nucleoside reverse transcriptase (RT) inhibitors (NNRTIs) have been previously shown to effectively inhibit wild-type (wt) and drug-resistant human immunodeficiency virus type 1 (HIV-1) replication. IASs proved to act through different mechanisms of action, depending on the nature and position of their chemical substituents. Here we describe selected novel IAS derivatives (*di-halo*-IASs). Our results show that these compounds are selective for the enzyme–substrate complex. The molecular basis for this selectivity was a different dissociation rate of the drug to a particular enzymatic form along the reaction pathway. By comparing the activities of the different compounds against wild-type RT and the resistant enzymes carrying the single mutations Lys103Asn, Leu100Ile, and Tyr181Ile (K103N, L100I, and Y181I), we found that one compound (RS1914) dissociated from the mutated enzymes almost 10-fold slower than from the wild type RT. These results demonstrate that IASs are very flexible molecules, interacting dynamically with the viral RT, and that this property can be successfully exploited to design inhibitors endowed with an enhanced binding to common NNRTI-resistant mutants.

1. Introduction

Anti-AIDS therapy is currently based on six classes of anti-human immunodeficiency virus (HIV) drugs. The nucleos(t)ide reverse transcriptase inhibitors (N(t)RTIs), the non-nucleoside reverse transcriptase inhibitors (NNRTIs), and the protease inhibitors (Beale and Robinson, 2000; Sluis-Cremer et al., 2000) are combined in the highly active antiretroviral therapy (HAART). In the past few years, new options for antiviral therapy have become available. In 2003, enfuvirtide, a 36-amino-acid residue peptide acting as a viral entry inhibitor, has been licensed for the treatment of HIV infection (Blasko, 2003; Jenny-Avital, 2003; Menzo et al., 2004; Oishi et al., 2008, Tomaras and Greenberg, 2001). In 2007, two new drugs, the entry inhibitor-CCR5 co-receptor antagonist maraviroc, and the integrase inhibitor raltegravir have been approved (Oversteegen et al., 2007). HAART regimens can achieve a major and prolonged reduction of viral replication, but they are unable to eradicate the viral infection. NNRTI-based HAART has become the first choice for initial antiviral therapy, because of their low toxicity and favorable pharmakinetics properties. However, the rapid emergence of drug resistance remains a pressing problem of NNRTIs. The need of agents effective against the drug-resistant mutants is a great stimulus for the research on new NNRTIs.

NNRTI interaction with HIV-1 reverse transcriptase (RT) is a highly dynamic process. Crystal structures of RT–NNRTI complexes showed that the drugs interacted with a hydrophobic pocket (non-nucleoside binding site [NNBS]) on the enzyme in a "butterfly-like" mode (Schäfer et al., 1993). One of the "wings" of this butterfly is made of a π-electron-rich moiety (phenyl or allyl substituents), that interacts through π–π interactions with a hydrophobic pocket, formed mainly by the side chains of aromatic amino acids (Tyr181, Tyr188, Phe227, Trp229, and Tyr318). On the other hand, the other wing is normally represented by a heteroaromatic ring, bearing at one side a functional group capable of donating and/or accepting hydrogen bonds with the main chain of Lys101 and Lys103. Finally, on the butterfly body, a hydrophobic portion fills a small pocket formed mainly by the side chains of Lys103, Val106, and Val179. Upon complexation, the NNBS hydrophobic pocket changes its own conformation, leading to the inactivation of the enzyme itself. NNBS adopts different conformations depending on the 3-D features of

* Corresponding author. Tel.: +39 0649913800; fax: +39 06491491.
** Corresponding author. Tel.: +39 0382 546354; fax: +39 0382 422286.
E-mail addresses: romano.silvestri@uniroma1.it (R. Silvestri), maga@igm.cnr.it (G. Maga).

0166-3542/$ – see front matter © 2008 Elsevier B.V. All rights reserved.
doi:10.1016/j.antiviral.2008.09.008

the inhibitors and the amino acids side chain flexibility. Moreover, mutations of some amino acids cause structural variations of the NNBS, which ultimately result in reduced affinities of most of the inhibitors (Patel et al., 1995; Patel and Preston, 1994). In particular, the NNRTI resistance mutations Tyr188Leu and Tyr181Ile/Cys reduce π–π interactions; the Gly190Ala mutation leads to a smaller active site space because of a steric conflict between the methyl side chain and the inhibitor and the formation of an additional hydrogen bond; when amino acid 103 is mutated from Lys to Asn it reduces inhibitor entrance into the NNBS (Ragno et al., 2005a,b). In addition, HIV-1 RT itself also undergoes a conformational reorganization upon interaction with its substrates template-primer (TP) and deoxynucleoside triphosphate (dNTP), so that three structurally distinct mechanistic forms can be recognized in the reaction pathway catalyzed by HIV-1 RT: the free enzyme, the binary complex of RT with the template primer (RT/TP), and the catalytically competent ternary complex of RT with both nucleic acid and dNTP (RT/TP/dNTP). This means that, in principle, the NNBS might not be identical in these three mechanistic forms (Crespan et al., 2005; Cancio et al., 2005). Several kinetic studies have shown that this is indeed the case, so that some NNRTIs selectively target one or a few of the different enzymatic forms along the reaction pathway. This observation likely reflects the different spatial rearrangements not only of the NNBS itself but also of the adjacent nucleotide binding site (Cancio et al., 2007; Crespan et al., 2005). Indeed, it has been shown that a "communication" exists between the NNBS and the nucleotide binding site, so that some NRTI resistance mutations can influence NNRTI binding and vice versa (Crespan et al., 2005). Thus, understanding the molecular determinants governing the selective interaction of a drug with the three different NNBS structures present along the RT reaction pathway, might be useful in designing novel, highly selective, and potent NNRTIs (De Martino et al., 2005). During extensive structure-activity relationship studies on sulfone NNRTIs, we identified potent pyrryl and indolyl aryl sulfones (IASs) (Silvestri and Artico, 2005; Silvestri et al., 2004). In particular, IAS derivatives bearing either 2-methylphenylsulfonyl or 3-methylphenylsulfonyl moieties at position 3 of the indole were found to inhibit HIV-1 at nanomolar concentrations. Furthermore, the introduction of a 3,5-dimethylphenylsulfonyl moiety led to compounds endowed with high activity and selectivity not only against the wild-type strain but also against the Tyr181Cys and Lys103Asn-Tyr181Cys viral variants and the efavirenz-resistant mutant Lys103Arg-Val179Asp-Pro225His (Silvestri et al., 2003).

In view of their extremely potent activities, especially towards NNRTI-resistant mutants, we sought to investigate in detail the mechanism of action of some selected IAS derivatives (Ragno et al., 2006). In a previous paper (Cancio et al., 2005), we have shown that IASs are highly flexible molecules, whose mode of interaction, and hence the mechanism of RT inhibition, can be modulated by the nature of the different substituents, so that from compounds endowed with a classical fully non-competitive mechanism, a series of inhibitors showing mixed-non-competitive and even partially competitive mechanism of action can be derived. This high flexibility was exploited to synthesise novel IAS derivatives able to better accommodate into the NNBS of drug resistant mutants.

In this work, we present the characterization of some *dihalo*-IAS derivatives endowed with nanomolar activities against HIV-1 RT wild type and mutated forms. We have already shown that the prototype compound of this class, RS1914, displayed subnanomolar activities against either laboratory strains or primary isolates of the HIV-1 virus wild type or carrying the Tyr181Cys mutation, and submicromolar activity against the double Tyr181Cys/Lys103Asn mutant virus (Regina et al., 2007). We have investigated their kinetic properties and show here that these compounds can selectively bind the RT enzyme, once complexed with its template/primer (TP) and substrates (dNTPs). Moreover, one compound, RS1914, showed an enhanced binding to the NNBS of the Lys103Asn and Tyr181Ile mutants, as revealed by a 10-fold slower dissociation rate from the mutated enzymes than from the wild type RT. These results demonstrate that IASs are very flexible molecules, interacting dynamically with the viral RT, and that this property can be successfully exploited to design inhibitors endowed with enhanced interaction with the NNRTI-resistant mutants.

2. Materials and methods

2.1. Chemicals

All the reagents were of analytical grade and purchased from Sigma–Aldrich (St. Louis, MO), Merck Sharp & Dohme (Readington, NJ), ICN (Research Products Division, Costa Mesa, CA), or AppliChem GmbH (Darmstadt, Germany). Radioactive 2′-deoxythymidine 5′-triphosphate [^{3}H]dTTP (40 Ci/mmol) was purchased from Amersham Bio-Sciences (GE Healthcare, Buckinghamshire, GB), while unlabeled dNTPs were from Boehringer Ingelheim GmbH (Ingelheim, Germany). GF/C filters were provided by Whatman Int. Ltd. (Maidstone, England).

2.2. Template/primer

The homopolymer poly(rA) and the oligomer oligo(dT)$_{12–18}$ (Pharmacia & Upjohn Inc. Pfizer, Peapack, NJ) were mixed at weight ratios in nucleotides of 10:1 with 25 mM Tris–HCl (pH 8.0) containing 22 mM KCl, heated at 70 °C for 5 min and then slowly cooled at room temperature.

2.3. Chemistry

Compounds. RS2723: *N*-{5-chloro-3-[(3,5-dimethylphenyl) sulfonyl]-4-fluoro-1*H*-indole-2-carbonyl}glycinamide; RS2913: 5-chloro-3-[(3,5-dimethylphenyl)sulfonyl]-4-fluoro-*N*-(2-(1*H*-pyrrol-1-yl)ethyl)-1*H*-indole-2-carboxamide; RS1914: 5-chloro-{3-[(3,5-dimethylphenyl)sulfonyl]-4-fluoro-1*H*-indole-2-carboxamide; RS2917: 5-chloro-3-[(3,5-dimethylphenyl)sulfonyl]-4-fluoro-*N*-(2-phenoxyethyl)-1*H*-indole-2-carboxamide (Fig. 1). Compounds RS2723, RS1914, were obtained by heating the corresponding esters with concentrated ammonium hydroxide in a sealed tube, or by treatment of the acid the corresponding amines in the presence of BOP reagent and triethylamine (RS2913 and 2917). The starting sulfone esters were obtained by oxidation of the corresponding 3-arylthio-1*H*-indole-2-carboxylates using 3-chloroperoxybenzoic acid (MCPBA). RS2723 was obtained by coupling reaction of 5-chloro-3-[(3,5-dimethylphenyl)sulfonyl]-4-fluoro-1*H*-indole-2-carboxylic acid in the presence of *O*-benzotriazol-1-yloxytris(dimethylamino)phosphonium hexafluorophosphate and triethylamine. The required 3-arylthio-1*H*-indole-2-carboxylates were prepared by reaction of proper arylthiodisulfides with 1*H*-indole-2-carboxylic acids in the presence of sodium hydride, according to the Atkinson method and subsequent esterification of the 3-arylthio-1*H*-indole-2-carboxylic acids with (trimethylsilyl)diazomethane. Alternatively, these esters were obtained by reaction of methyl or ethyl 1*H*-indole-2-carboxylates with *N*-(arylthio)succinimides in the presence of boron trifluoride diethyl etherate (Ragno et al., 2006; Regina et al., 2007; Silvestri and Artico, 2005; Silvestri et al., 2003).

2.4. Expression, purification and cloning of recombinant HIV-1 RT forms

Recombinant heterodimeric RT, either wild-type or the Lys103Asn, Leu100Ile and Tyr181Ile variants were expressed and purified as briefly described below.

The HIV-1 RT gene fragment spanning codons 2–261 from pHXB2D2-261RT constructs carrying K103N, L100I and Y181I mutations was amplified by PCR, digested with Acc1 and Pvu2 and cloned into the expression plasmid p6HRT (ΔXho1/Bgl2), containing the wild type RT gene. The resulting p6HRT expression vectors with K103N, L100I and Y181I mutations were used for the production in E. coli (BL21) and purification of recombinant His-tagged RT enzymes in a Fast Protein Liquid Chromatography (F-PLC) system, using Ni-NTA superflow column (QIAGEN) (Abdullah and Chase, 2005). All the enzymes were purified to a >95% purity, as confirmed by sodium dodecyl sulfate-polyacrylamide gel electrophoresis and Gelcode Blue stain, and had a specific activity on poly(rA):oligo(dT). One Unit of DNA polymerase activity corresponds to the incorporation of 1 nmol of dNMP into acid-precipitable material in 60 min at 37 °C.

Western Blotting confirmed the identity of the polypeptides present in the final preparation with anti-RT monoclonal antibodies.

2.5. HIV-1 RT RNA-dependent DNA polymerase activity assay

Poly(rA)/oligo(dT) was used as a template for the RNA-dependent DNA polymerase reaction by HIV-1 RT, either wt or mutant. For the activity assay, a 25 μl final reaction volume contained TDB buffer (50 mM Tris–HCl (pH 8.0), 1 mM dithiothreitol (DTT), 0.2 mg/ml bovine serum albumine (BSA), 2% glycerol), 10 mM $MgCl_2$, 0.5 mg of poly(rA):oligo(dT)$_{10:1}$ (0.3 μM 3′-OH ends), 10 μM [^{3}H]dTTP 1 Ci/mmol and, finally, introduced into tubes containing aliquots of different enzyme concentrations (5–10 nM RT). After incubation at 37 °C for the indicated time, 20 μL from each reaction tube were spiked on glass fiber filters GF/C and, immediately, immersed in 5% ice-cold trichloroacetic acid (TCA) (AppliChem GmbH, Darmstadt). Filters were washed three times with 5% TCA and once with ethanol for 5 min, then dried and, finally, added to EcoLume® Scintillation cocktail (ICN, Research Products Division, Costa Mesa, CA), to detect the acid-precipitable radioactivity by PerkinElmer® Trilux MicroBeta 1450 Counter.

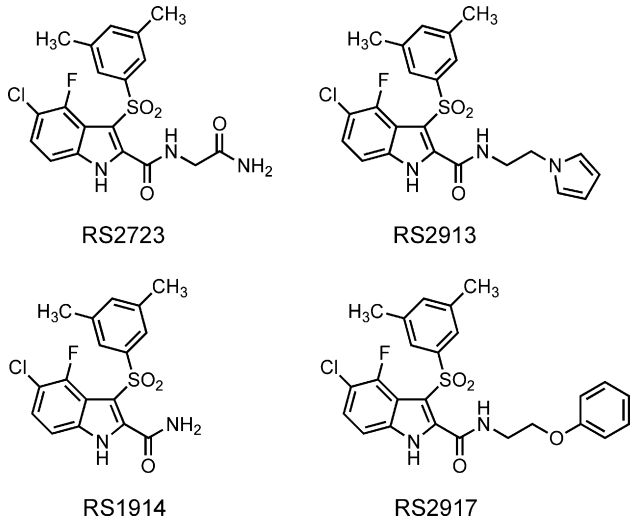

Fig. 1. Structures of the compounds used in this study.

2.6. Steady-state kinetic assays

Steady state kinetic assays were also performed to evaluate the activity of HIV-1 RT in the presence of fixed concentrations (ID_{50}), of selected inhibitors and variable concentrations of either poly(rA)/oligo(dT) or [^{3}H]TTP, while the other was maintained at saturating doses. [^{3}H]TTP concentrations varied between 0.2 and 20 μM, while poly(rA)/oligo(dT) doses ranged from 10 to 200 nM. These experiments led to the determination of V_{max}, K_m and k_{cat} parameters from Michaelis Menten curves, as mentioned in the "calculation of kinetic parameters" section. The true inhibitor dissociation constant (K_i) values were derived as described.

2.7. Kinetics of inhibitor binding

Kinetics of inhibitor binding experiments were as described previously. Briefly, HIV-1 RT (20–40 nM) was incubated for 2 min at 37 °C in a final volume of 4 μl in the presence of TDB buffer, with 10 mM $MgCl_2$ alone or with 100 nM 3′-OH ends (for the formation of the RT/TP complex), or in the same mixture complemented with 10 μM unlabeled dTTP (for the formation of the RT/TP/dNTP complex). The inhibitor to be tested was then added to a final volume of 5 μl at a concentration at which $[EI]/[E_0] = [1 - 1/(1 + [I]/K_i)] > 0.9$. Then, 145 μl of a mix containing TDB buffer, 10 mM $MgCl_2$, and 10 μM [^{3}H]dTTP (5 Ci/mmol) was added at different time points. After an additional 10 min of incubation at 37 °C, 50-μl aliquots were spotted on GF/C filters, and acid-precipitable radioactivity was measured as described for the HIV-1 RT RNA-dependent DNA polymerase activity assay. The v_t/v_0 ratio, representing the normalized difference between the amount of dTTP incorporated at the zero time point and at different time points, was then plotted against time. The k_{app} values, the association rate (k_{on}) and the dissociation rate (k_{off}) values were calculated as described in the kinetic parameter calculation section.

2.8. Kinetic model

The mechanism of action of these *di-halo*-IASs was found to be either fully non-competitive or partially mixed. A schematic drawing of the different equilibria is depicted in Fig. 2. According to the ordered mechanism of the polymerization reaction, whereby template-primer (TP) binds first followed by the addition of dNTP, HIV-1 RT can be present in three different catalytic forms as reported in Fig. 2A: as a free enzyme, in a binary complex with the TP, and in a ternary complex with TP and dNTP. The resulting rate equation for such a system is very complex and impractical to use. For these reasons, the general steady-state kinetic analysis was simplified by varying one of the substrates (either TP or dNTP) while the other was kept constant. When the TP substrate was held constant at saturating concentration and the inhibition at various concentrations of dNTPs was analyzed, at the steady-state all of the input RT was in the form of the RT/TP binary complex and only two forms of the enzyme (the binary complex and the ternary complex with dNTP) could react with the inhibitor, as shown in the left part of Fig. 2. Similarly, when the dNTP concentration was kept constant at saturating levels and the inhibition at various TP concentrations was analyzed, RT was present either as a free enzyme or in the ternary complex with TP and dNTP, as shown in the right part of Fig. 2.

The steady-state rate equation used for the partially mixed inhibition was the one describing a reaction involving only two

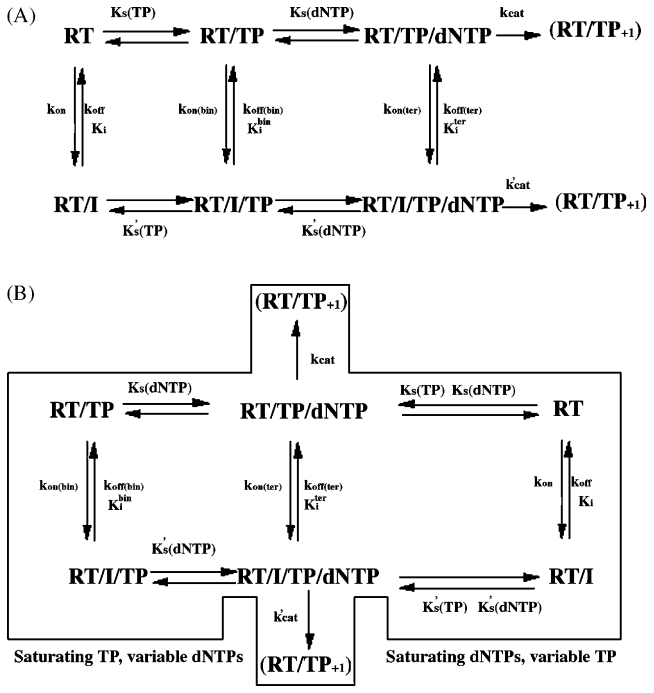

Fig. 2. Simplified kinetic pathway for the reaction catalysed by HIV-1 RT and its interaction with inhibitors. (A) Schematic representation of the different equilibria in the reaction catalysed by HIV-1 RT in the absence or in the presence of an inhibitor. TP, template/primer; dNTP, nucleoside triphosphate; *I*, inhibitor; K_m, Michelis constant relative to the different substrates; k_{cat}, apparent catalytic rate; k_{off}, dissociation rate; k_{on}, association rate; K_i, equilibrium dissociation constant of the inhibitor; bin, binary complex of the enzyme with the TP substrate; ter, ternary complex of the enzyme with the TP and dNTP substrates. (B) Simplified reaction pathway under the reaction conditions used in this study. For details see text.

mechanistic forms of the enzyme (according to the simplified pathways in Fig. 2B).

2.9. Data analysis and statistics

Data obtained were analyzed by non-linear regression analysis using GraphPad Software (San Diego, CA, USA).

2.10. Kinetic parameter calculation

All values were calculated by non-least-squares computer fitting of the experimental data to the appropriate rate equations.

Steady-state inhibitor binding was analysed according to the equation for mixed type inhibition:

$$v = \left\{ \frac{[V_{max}/(1 + I/K_i'')]}{[1 + (K_m/S)]} \frac{(1 + I/K_i')}{(1 + I/(K_i''))} \right\} \quad (1)$$

According to Fig. 2B, when TP was saturating, left part, $K_i' = K_i^{free}$, whereas at saturating dNTP (right part), $K_i' = K_i^{bin}$. In all cases, $K_i'' = K_i^{ter}$. According to the mixed-type mechanism of Eq. (1) it follows that, if $K_i' = K_i''$, then both K_m and V_{max} values will decrease at increasing inhibitor concentrations. When $K_i' = K_i''$, then Eq. (1) can be simplified to the one describing a fully non-competitive mechanism.

The equilibrium dissociation constants (K_i' and K_i'') were calculated under the conditions shown in Fig. 2B, right panel, from the variations of the K_m and V_{max} values as a function of the inhibitor concentrations according to the equations:

$$K_i' = \frac{I}{\{[K_p(1 + I/K_i')/K_m] - 1\}} \quad (2)$$

$$K_i'' = \frac{I}{[(V_{max}/V_p) - 1]} \quad (3)$$

where K_p and V_p are the apparent K_m and V_{max} values, respectively, at each given inhibitor concentration.

The true inhibition constant K_i (which according to the kinetic model was assumed as $K_i^{bin} = K_i^{ter}$) was calculated under the conditions shown in Fig. 2B, left panel.

The apparent catalytic rates were calculated from the relationship: $v_0 = k_{cat}[E]_0$

The apparent binding rate (k_{app}) values were determined by fitting the experimental data to the single-exponential equation:

$$\frac{v_t}{v_0} = e^{-k\ app^t} \quad (4)$$

where *t* is time. If $[E]_0$ is the input enzyme concentration, $[E]_t$ is the enzyme available for the reaction at time *t*, and $[E{:}I]_t$ is the enzyme bound to the inhibitor at time *t*, it follows that

$$[E]_t = [E]_0 - [E : I]_t$$

Since $v_0 = k_{cat}[E]_0$ and $v_t = k_{cat}[E]_t$, then $v_t/v_0 = 1 - [E{:}I]_t/[E]_0$. Thus, the v_t/v_0 value is proportional to the fraction of enzyme bound to the inhibitor.

The true association (k_{on}) and dissociation (k_{off}) rates were calculated from the equations:

$$k_{app} = k_{on}([I] + K_i) \quad (5)$$

$$k_{off} = k_{on}K_i \quad (6)$$

3. Results

3.1. Di-halo-IAS are mixed-type inhibitors of HIV-1 RT, with higher affinity for the enzyme–substrate complexes

In order to determine the exact mechanism of action of these compounds, the RNA dependent DNA polymerase activity of HIV-1 RT, either wild type or mutated (K103N, L100I and Y181I) was measured in the absence or in the presence of fixed concentrations of the inhibitors and variable concentrations of either the nucleic acid (template/primer) and/or nucleotide substrate, respectively, while the other was maintained at saturating concentrations. The corresponding equilibria are illustrated in Fig. 2. Data were interpolated and the K_m, and V_{max} values (Table 1) were calculated according to Section 2. Interestingly, we found that both the K_m and the V_{max} values obtained varying the nucleic acid substrate concentrations were significantly decreased as the inhibitor concentration increased (Fig. 3A and B). On the other hand, when the nucleotide substrate concentration was varied, only the V_{max} showed a dose-dependent reduction by the tested IAS derivatives (Fig. 3C), whereas the K_m did not change (Fig. 3D). The equilibrium dissociation constants for the inhibitors (K_i) from the different enzymatic forms along the reaction pathway (free enzyme, binary complex with the nucleic acid (template/primer) and ternary complex with both the nucleic acid (template/primer) and the nucleotide substrate) were calculated from the variations of the V_m and K_m values (see Section 2) according to the simplified kinetic pathway shown in Fig. 2. The corresponding values are listed in Table 1. Thus, the IAS derivatives behaved as mixed-type inhibitors, showing higher affinity for the binary RT/TP and ternary RT/TP/dNTP complexes than for the free enzyme ($K_i^{free} > K_i^{bin} \approx K_i^{ter}$). The true inhibition constant (K_i)

Table 1
Equilibrium dissociation constants (K_i) values of the IAS compounds, along with nevirapine and efavirenz, with respect to the different eznymatic forms of HIV-1 RT wild type and mutants.

Compound	WT		K103N		L100I		Y181I	
	K_i^{free} (μM)[a]	$K_i^{bin/ter}$ (μM)	K_i^{free} (μM)	$K_i^{bin/ter}$ (μM)	K_i^{free} (μM)	$K_i^{bin/ter}$ (μM)	K_i^{free} (μM)	$K_i^{bin/ter}$ (μM)
RS 2723	0.031[b] (±0.003)	0.025 (±0.002)	3.5 (±0.3)	1.42 (±0.12)	1.5 (±0.1)	0.55 (±0.055)	3.6 (±0.3)	2.6 (±0.26)
RS 2913	0.04 (±0.005)	0.018 (±0.002)	0.7 (±0.04)	0.17 (±0.017)	0.1 (±0.01)	0.03 (±0.003)	7.5 (±0.5)	3.7 (±0.37)
RS 2917	0.07 (±0.008)	0.006 (±0.001)	1.2 (±0.2)	0.36 (±0.036)	0.2 (±0.03)	0.03 (±0.003)	15 (±1)	8.4 (±0.840)
RS 1914	0.058 (±0.006)	0.003 (±0.0005)	0.07 (±0.01)	0.006 (±0.001)	0.01 (±0.002)	0.002 (±0.0003)	0.2 (±0.03)	0.029 (±0.003)
NVP	0.4 (±0.05)	0.4 (±0.04)	3.3 (±0.3)	5 (±0.05)	7 (±0.05)	9 (±0.9)	34 (±2)	36 (±2)
EFV	0.03 (±0.006)	0.004 (±0.001)	1.5 (±0.2)	0.2 (±0.03)	0.15 (±0.01)	0.02 (±0.003)	0.9 (±0.1)	0.12 (±0.02)

[a] free, free enzyme; bin, binary complex; ter, ternary complex. For a schematic diagram of the reaction, see Fig. 2.
[b] Values are the mean of three independent replicates ±S.D.

was then considered as the one corresponding to the equilibrium dissociation constant from the ternary complex (K_i^{ter}).

3.2. Effect of NNRTI resistance mutations on di-halo-IAS inhibition activity

In order to elucidate the influence of the Lys103Asn, Leu100Ile and Tyr181Ile mutations on the activity of each di-halo-IAS examined, we calculated the ratio between the inhibitory potencies against the mutated RT forms (K_i^{ter} mut) and against the RT wild type (K_i^{ter} wt) (Table 1). This ratio (K_i^{ter} mut/K_i^{ter} wt), referred as relative resistance index (RRI), measures the degree at which the selected mutation reduced the affinity of the enzyme for the inhibitor, the higher the RRI value, the lower the affinity for the mutant with respect to the wild type enzyme. RRI comparison for all the inhibitors tested is shown in Fig. 4. It can be seen that the Tyr181Ile mutation caused the highest decrease in the inhibitory potencies for all the compounds tested (Fig. 4A), whereas the mutation Leu100Ile only marginally affected the affinity of the enzyme for the IAS derivatives (Fig. 4B). Compound RS1914 was the least affected by all the mutations, showing a 9.7-fold decrease in potency against the Tyr181Ile mutant (Fig. 4B), and only a 2-

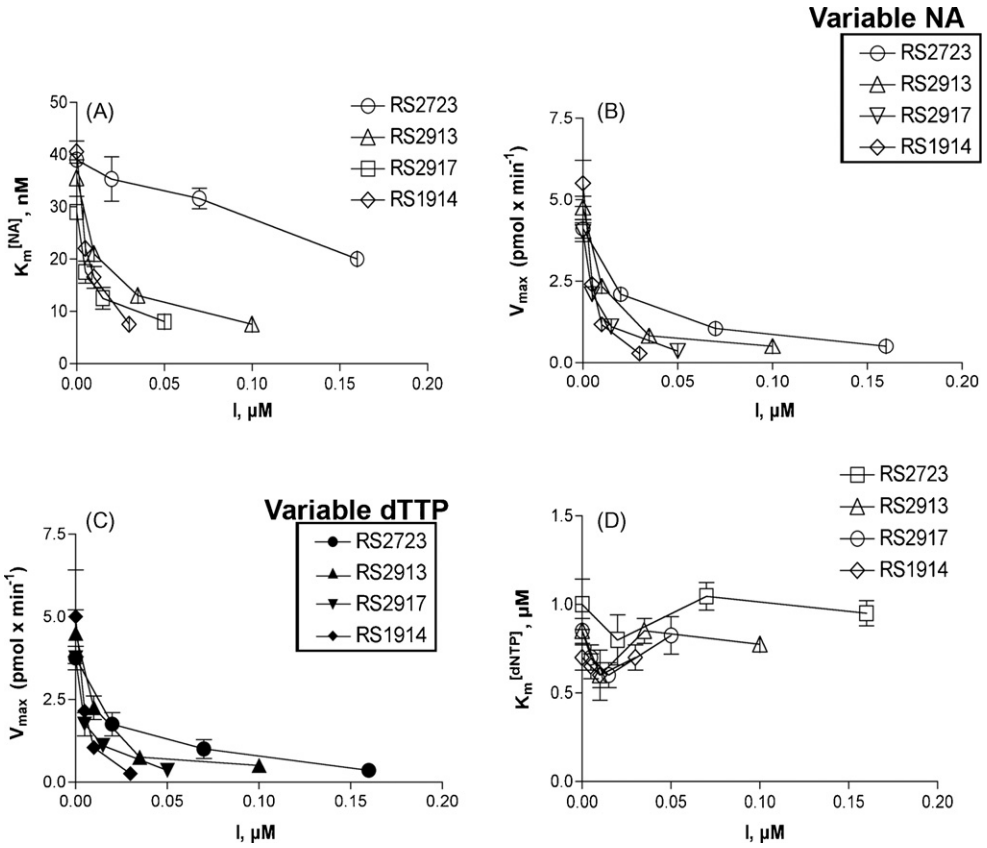

Fig. 3. Di-halo-IAS are mixed-type inhibitors of HIV-1 RT wild type. (A) Variation of the apparent affinity (K_m) for the nucleic acid (NA) substrate as a function of the inhibitor concentration. Values are the mean of three independent estimates. Error bars are ±S.D. (B) Variation of the apparent maximal velocity (V_{max}) of the reaction as a function of the inhibitor concentration at variable nucleic acid concentrations. Values are the mean of three independent estimates. Error bars are ±S.D. (C) Variation of the apparent maximal velocity (V_{max}) of the reaction as a function of the inhibitor concentration at variable dTTP concentrations. Values are the mean of three independent estimates. Error bars are ±S.D. (D) Variation of the apparent affinity (K_m) for the nucleotide (dNTP) substrate as a function of the inhibitor concentration. Values are the mean of three independent estimates. Error bars are ±S.D.

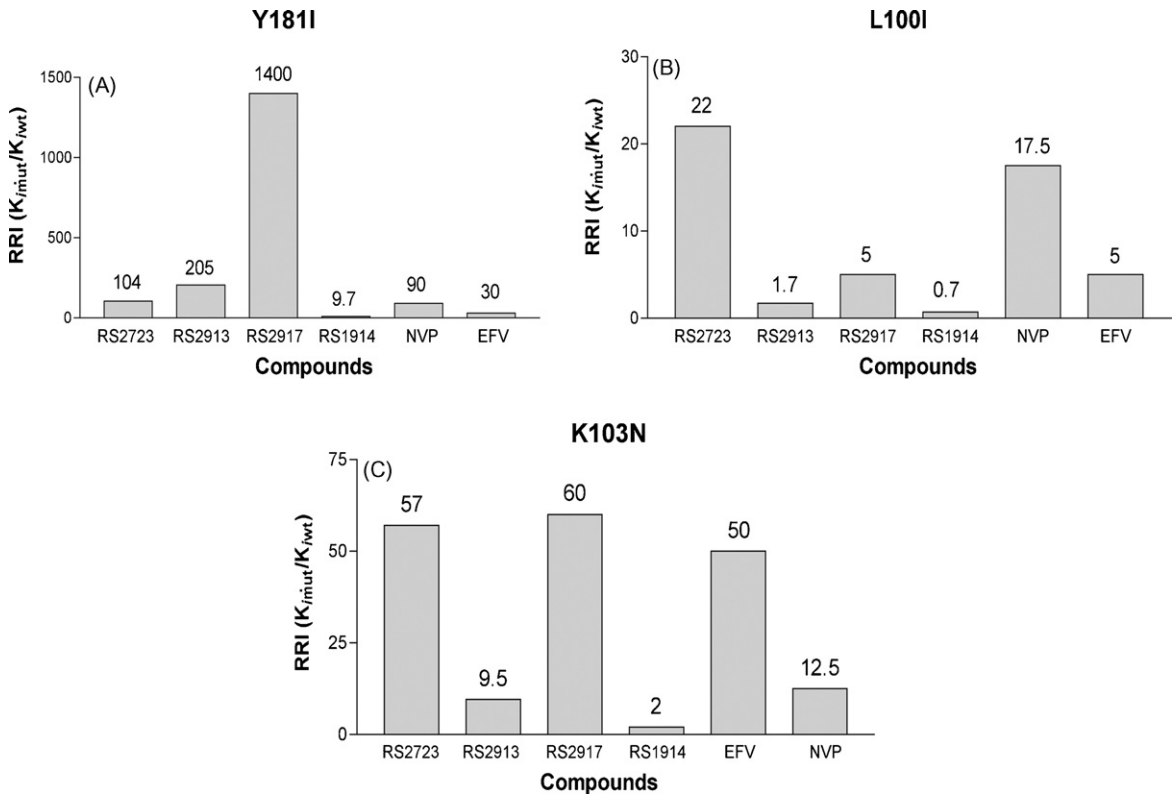

Fig. 4. RS2913 and RS1914 show high levels of activity towards drug resistant mutants and faster association rates to the binary/ternary complex of HIV-1 RT than to the free enzyme. (A) Relative resistance indexes of the different compounds towards the mutant Tyr181Ile (Y181I); EFV, efavirenz, NVP, nevirapine. (B) Relative resistance indexes of the different compounds towards the mutant Leu100Ile (L100I); EFV, efavirenz, NVP, nevirapine. C. Relative resistance indexes of the different compounds towards the mutant Lys103Asn (K103N); EFV, efavirenz, NVP, nevirapine.

fold decrease against the Lys103Asn mutant (Fig. 4C), whereas it was unaffected by the Leu100Ile mutant (RRI ≈ 1, Fig. 4B). The activity of the other compounds, on the other hand, was found to be dependent on both the nature of the substituents and the particular mutation analyzed. For example, compounds RS2723 and RS2917, showed a comparable (≈60-fold) loss of potency towards the Lys103Asn mutant (Fig. 4C). However, RS2723 was 5-fold more affected than RS2917 by the Leu100Ile mutation (Fig. 4B), whereas RS2917 showed a 12-fold higher reduction of activity than RS2723 against the Tyr181Ile mutant (Fig. 4A). However, when compared to the clinically used compounds nevirapine (NVP) and efavirenz (EFV), the IAS derivative RS1914 showed a significantly improved resistance profile towards all the tested mutants (Fig. 4A–C).

3.3. The higher affinity of the IAS derivatives to the complex of RT with its substrates is driven by a faster association rate

In order to clarify the molecular mechanisms for observed mixed-type inhibition exhibited by the IAS inhibitors towards the RT mutants, we evaluated, for the most active compounds RS1914 and RS2913, the corresponding association (k_{on}) and dissociation (k_{off}) rates for the three forms of the HIV-1 RT along the reaction pathway (Fig. 2), namely the free enzyme, the binary complex of RT with the nucleic acid substrate and the ternary complex of RT with both the nucleic acid and the nucleotide substrates. The calculated values are summarized in Table 2. Fig. 5A shows a comparison of the k_{on} and k_{off} values of both compounds for the different enzymatic forms of HIV-1 RT wild type. It can be seen that both compounds showed significantly higher association rates for the binary and ternary complex with respect to the free enzyme, whereas k_{off} values were only slightly different among the different enzymatic forms. These data indicate that the NNBS of HIV-1 RT is more accessible to the IAS derivatives when the enzyme is in complex with its template/primer and substrate, thus explaining the mixed-type mechanism of inhibition observed with these analogs.

3.4. RS1914 shows tighter binding to RT carrying NNRTI-resistance mutations than to the wild type enzyme

Since the equilibrium dissociation constant K_i is related to these velocities by the relationship $K_i = k_{off}/k_{on}$, a reduced affinity (corresponding to an increase of the K_i value) may be associated to a decrease in k_{on} (slower association) or to an increase in k_{off} (faster dissociation). The association and dissociation rates for the ternary complexes (k_{on}^{ter} and k_{off}^{ter}) were used to calculate the relative association index (RAI = k_{on}^{ter} wt/k_{on}^{ter} mut) and the relative dissociation index (RDI = k_{off}^{ter} mut/k_{off}^{ter} wt) for the most active compounds RS1914 and RS29133. With RAI or RDI values >1, the inhibitor either shows a lower association rate to the mutated enzyme than to the wild type or dissociates more rapidly, the complex formed by the mutant and the inhibitor being unstable. In the case of RAI or RDI values <1, the opposite reasoning holds, revealing a selectivity of the inhibitor to the mutant enzymes. The results are shown in Fig. 5. Both the Tyr181Ile and the Lys103Asn mutations significantly decreased the association rates of the compounds to the mutated enzymes (Fig. 5B). The clinically relevant compounds EFV and NVP, also showed similar reductions in their association rates with the Lys103Asn mutant. On the other hand, interesting data emerged from RDI value analysis: RS1914 showed RDI < 1 towards

Table 2
Kinetic parameters for the interaction of IAS derivatives with HIV-1 RT wild type and drug resistant mutants.

	[*E*]^a			[*E*:NA]			[E:DNA:dTTP]		
	RT wt								
	K_i^{free} (μM)^b	k_{on} (s^{-1} μM^{-1}) × 10^2	k_{off} (s^{-1}) × 10^2	K_i^{bin} (μM)	k_{on} (s^{-1} μM^{-1}) × 10^2	k_{off} (s^{-1}) × 10^2	K_i^{ter} (μM)	k_{on} (s^{-1} μM^{-1}) × 10^2	k_{off} (s^{-1}) × 10^2
RS 1914	0.058 (±0.001)	14.3 (±0.7)	0.83 (±0.08)	0.003 (±0.0005)	79 (±7)	0.24 (±0.024)	0.003 (±0.0005)	176 (±17)	0.53 (±0.053)
RS 2913	0.04 (±0.004)	9.8 (±0.8)	0.39 (±0.038)	0.018 (±0.002)	13.7 (±0.8)	0.23 (±0.023)	0.018 (±0.002)	27.2 (±0.7)	0.45 (±0.045)
EFV[c]	0.03(±0.008)	1(±0.1)	0.03(±0.01)	0.03(±0.007)	1(±0.1)	0.03(±1)	0.004(±0.001)	4(±0.2)	0.016(±0.3)
NVP	0.4(±0.06)	0.4(±0.1)	0.16(±0.01)	0.5(±0.1)	0.3(±0.02)	0.15(±0.01)	0.4(±0.08)	0.4(±0.1)	0.16(±0.01)
	K103N								
RS 1914	0.07 (±0.001)	7.5 (±0.87)	0.52 (±0.005)	0.006 (±0.001)	84 (±8)	0.51 (±0.05)	0.006 (±0.001)	9.4 (±0.94)	0.057 (±0.006)
RS 2913	0.7 (±0.034)	0.4 (±0.07)	0.28 (±0.022)	0.170. (±0.017)	3.2 (±0.3)	0,54 (±0.054)	0.17 (±0.017)	3.91 (±0.39)	0.66 (±0.067)
EFV	1.5(±0.2)	0.2(±0.03)	0.3(±0.03)	1.6(±0.3)	0.25(±0.05)	0.4(±0.05)	0.2(±0.01)	0.6(±0.01)	0.12(±0.01)
NVP	3.3(±0.2)	0.03(±0.005)	0.1(±0.02)	3.3(±0.2)	0.03(±0.005)	0.1(±0.02)	5(±0.5)	0.03(±0.005)	0.15(±0.01)
	Y181I								
RS 1914	0.2 (±0.03)	0.1 (±0.01)	0.02 (±0.002)	0.029 (±0.003)	0.38 (±0.04)	0.011 (±0.001)	0.029 (±0.003)	2.1 (±0.2)	0.061 (±0.006)
RS 2913	7.5 (±0.7)	0.05 (±0.01)	0.37 (±0.037)	3.7 (±0.37)	0.87 (±0.09)	3.2 (±0.3)	3.7 (±0.37)	0.12 (±0.01)	0.44 (±0.044)

[a] [*E*], free enzyme; [*E*:NA], binary complex with nucleic acid; [*E*:NA:dNTP], ternary complex with nucleic acid and nucleotide.
[b] Values are the means of three independent replicates ±S.D.
[c] EFV, efavirenz,; NVP, nevirapine.

both K103N and Y181I, indicating a significantly (≈10-fold) slower dissociation rate from both the mutant enzymes than from wild type RT (Fig. 5C). As a result, the compound RS1914 dissociated from the Lys103Asn mutant 75-fold and 10-fold more slowly than the reference compounds EFV and NVP, respectively. With RS 2913, the k_{off} for Lys103Asn was only 1.5-fold higher than the k_{off} for RT wt, whereas this compound disassociated from both the mutant Tyr181Ile and RT wild type at the same rate, the corresponding RDI value being ≈1.

4. Discussion

In the present work, we expand our previous investigations on the mechanism of action of IAS derivatives. We have previously shown that the nature and position of the substituents on the drug pharmacophore can influence the selective interaction of the compound with different mechanistic forms of the viral RT. During extensive structure-activity relationship studies, we identified *di-halo*-IASs as novel highly potent NNRTIs (Silvestri and Artico, 2005). In particular, IAS derivatives bearing two halogen atoms (chlorine and fluorine, respectively at positions 4 and 5 of the indolyl nucleus) as well as two methyl groups at positions 3 and 5 of the phenylsulfonyl moiety, were found to inhibit HIV-1 at nanomolar concentrations, and displayed high activity and selectivity not only against the wild-type strain but also against the Tyr181Ile and Lys103Asn NNRTI-resistant mutants (Regina et al., 2007). In this work, we showed that the *di-halo*-IAS RS2723, RS2913, RS2917 and RS1914 interact dynamically with the viral RT and selectively bind to the enzyme in complex with its template/primer and substrate. Except for RS1914 which is a primary carboxamide, the other three compounds bear different side chains at the 2-carboxamide function, as illustrated in Fig. 1. The results of our kinetic analysis showed that all these compounds have higher association rates (k_{on}) to the binary and ternary complexes than to the free enzyme. One compound, RS1914, retained high inhibitory activity towards all the mutants tested, with K_i values ranging between 0.003 and 0.03 μM. This high activity is reflected by the very low resistance indexes, which ranged from 0.7 to 9.7. In particular, RS1914 showed a much better activity profile than the reference compounds NVP and EFV towards all the clinically relevant mutants analysed. We have already shown that RS1914 displayed subnanomolar activities against either laboratory strains or primary isolates of the HIV-1 virus wild type or carrying the Tyr181Cys mutation, and submicromolar activity against the double Tyr181Cys/Lys103Asn mutant virus (Regina et al., 2007). The kinetic analysis presented here elucidates the molecular basis for the high activity of RS1914. In fact, comparison of the association and dissociation rates between RT wild type and the mutant forms, demonstrated that this primary carboxamide displayed the highest association and the slowest dissociation rates to the mutated RT forms. Moreover, RS1914 showed a ≈10-fold lower dissociation rate from the mutant forms Lys103Asn and Tyr181Ile than from the wild type RT, implying an enhanced binding selectivity to the mutated NNBS. These data further indicate that IAS compounds are very flexible molecules, which are able to adapt their conformation in order to achieve an optimal interaction with the NNBS even in the presence of mutations such as Lys103Asn and Tyr181Ile, which are invariably associated with high level resistance to all the clinically used NNRTIs. Our kinetic data suggest that the affinity of the *di-halo*-IAS inhibitors to HIV-1 RT is dictated by the nature of the functional group at position 2 of the indole ring. The reduced binding and/or faster dissociation relative to the mutated forms, especially Tyr181Ile, which was observed for those inhibitors with bulkier substituents at that position with respect to RS1914, might be due to steric clashes which obstruct

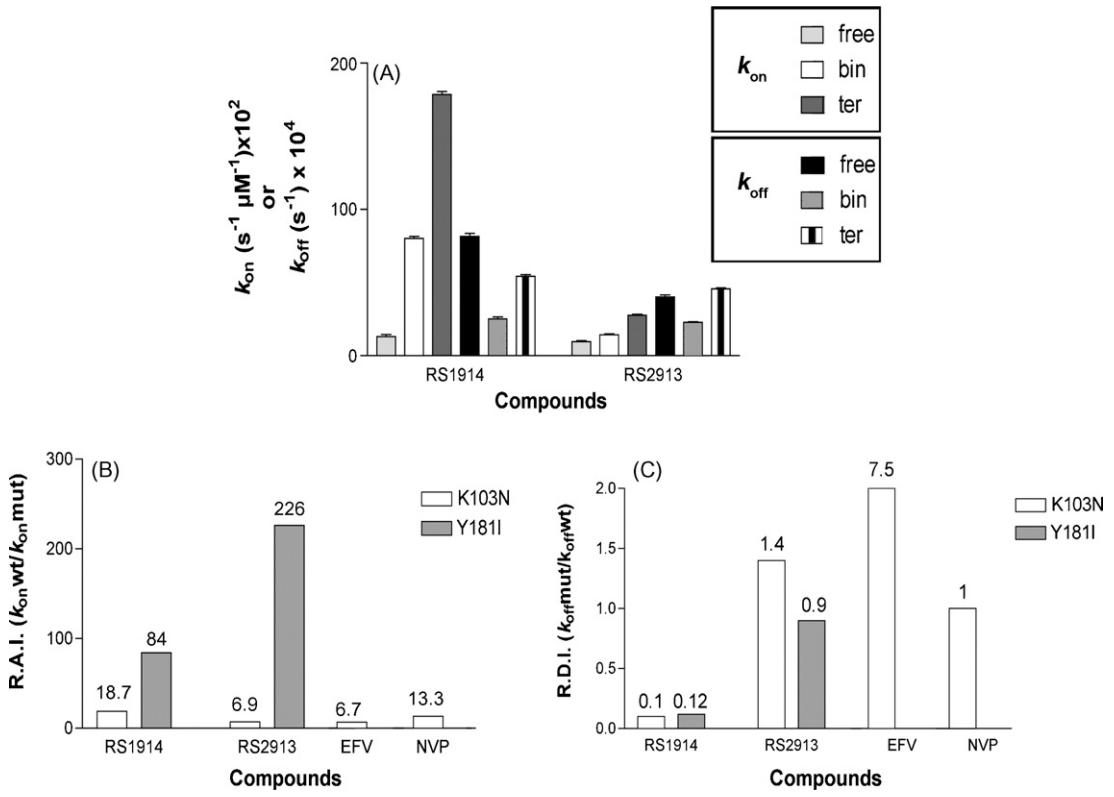

Fig. 5. Compound RS1914 dissociates from the drug resistant mutant RT enzymes at a slower rate than from the wild type enzyme. (A) Comparison of the association (k_{on}) and dissociation (k_{off}) rates of compounds RS1914 and RS2913 for the free enzyme, the binary complex and the ternary complex of HIV-1 RT wild type. (B) Relative association indexes of compounds RS1914, RS2913, nevirapine (NVP) and efavirenz (EFV) for the Lys103Asn (K103N) mutant (white bars) and of compounds RS1914, RS2913 for the Tyr181Ile (Y181I) mutant (grey bars) RT. (C) Relative dissociation indexes of compounds RS1914, RS2913, nevirapine (NVP) and efavirenz (EFV) for the Lys103Asn (K103N) mutant (white bars) and of compounds RS1914, RS2913 for the Tyr181Ile (Y181I) mutant (grey bars) RT.

the entrance of the inhibitor into the NNBS pocket and/or reduce the stability of the complex formed.

5. Conclusions

In conclusion, by targeting the enzyme-substrate complexes, the *di-halo*-IAS RS1914 showed improved activity towards the Tyr181Ile mutant enzyme and comparable activity towards the Lys103Asn mutant RT in comparison with the previously characterized IAS derivatives (Cancio et al., 2007), which preferentially associated with the free enzymatic form of HIV-1 RT. In addition, RS1914 showed much slower dissociation rates from both mutant enzymes with respect to HIV-1 RT wild type and showed a superior activity profile towards the Lys103Asn, Leu100Ile and Tyr181Ile mutants with respect to the reference compounds NVP and EFV. The results obtained by this study, as well as the excellent activity demonstrated by these inhibitors in blocking the viral replication in infected cells, suggest a possible use of these compounds for the therapy of HIV. Therefore, further toxicity and pharmacokinetics studies are warranted.

Acknowledgements

This work has been partially supported by the VI National Program AIDS Grant n.40G.36 and by the EU grant LSHP-CT-2006-037257 Excellent to GM. GLR., FP and RS thank the financial support of the Italian MUR (PRIN 2006 - Prot. no. 2006030809), and Istituto Pasteur - Fondazione Cenci Bolognetti. SZ is a recipient of a Buzzati-Traverso Fellowship. AK is a recipient of a Fellowship from the Italian Ministery of Foreign Affairs.

References

Abdullah, N., Chase, H.A., 2005. Removal of poly-histidine fusion tags from recombinant proteins purified by expanded bed adsorption. Biotechnol. Bioeng. 92, 501–513.

Beale, K.K., Robinson Jr., W.E., 2000. Combinations of reverse transcriptase, protease, and integrase inhibitors can be synergistic in vitro against drug-sensitive and RT inhibitor-resistant molecular clones of HIV-1. Antiviral Res. 46, 223–232.

Blasko, M., 2003. HIV-1 fusion inhibitor improves treatment in HIV-1-resistant patients. Dtsch. Med. Wochenschr. 128, 1032.

Cancio, R., Silvestri, R., Ragno, R., Artico, M., De Martino, G., La Regina, G., Crespan, E., Zanoli, S., Hubscher, U., Spadari, S., Maga, G., 2005. High potency of indolyl aryl sulfone nonnucleoside inhibitors towards drug-resistant human immunodeficiency virus type 1 reverse transcriptase mutants is due to selective targeting of different mechanistic forms of the enzyme. Antimicrob. Agents Chemother. 49, 4546–4554.

Cancio, R., Mai, A., Rotili, D., Artico, M., Sbardella, G., Clotet-Codina, I., Este, J.A., Crespan, E., Zanoli, S., Hubscher, U., Spadari, S., Maga, G., 2007. Slow-tight-binding HIV-1 reverse transcriptase non-nucleoside inhibitors highly active against drug-resistant mutants. ChemMedChem. 2, 445–448.

Crespan, E., Locatelli, G.A., Cancio, R., Hubscher, U., Spadari, S., Maga, G., 2005. Drug resistance mutations in the nucleotide binding pocket of human immunodeficiency virus type 1 reverse transcriptase differentially affect the phosphorolysis-dependent primer unblocking activity in the presence of stavudine and zidovudine and its inhibition by efavirenz. Antimicrob. Agents Chemother. 49, 342–349.

De Martino, G., La Regina, G., Di Pasquali, A., Ragno, R., Bergamini, A., Ciaprini, C., Sinistro, A., Maga, G., Crespan, E., Artico, M., Silvestri, R., 2005. Novel 1-[2-(diarylmethoxy)ethyl]-2-methyl-5-nitroimidazoles as HIV-1 non-nucleoside reverse transcriptase inhibitors. A structure-activity relationship investigation. J. Med. Chem. 48, 4378–4388.

Jenny-Avital, E.R., 2003. Enfuvirtide, an HIV-1 fusion inhibitor. N. Engl. J. Med. 349, 1770–1771.

Menzo, S., Castagna, A., Monachetti, A., Hasson, H., Danise, A., Carini, E., Bagnarelli, P., Lazzarin, A., Clementi, M., 2004. Genotype and phenotype patterns of human immunodeficiency virus type 1 resistance to enfuvirtide during long-term treatment. Antimicrob. Agents Chemother. 48, 3253–3259.

Oishi, S., Ito, S., Nishikawa, H., Watanabe, K., Tanaka, M., Ohno, H., Izumi, K., Sakagami, Y., Kodama, E., Matsuoka, M., Fujii, N., 2008. Design of a novel HIV-1 fusion inhibitor that displays a minimal interface for binding affinity. J. Med. Chem. 51, 388–391.

Oversteegen, L., Shah, M., Rovini, H., 2007. HIV combination products. Nat. Rev. Drug Discov. 6, 951–952.

Patel, P.H., Preston, B.D., 1994. Marked infidelity of human immunodeficiency virus type 1 reverse transcriptase at RNA and DNA template ends. Proc. Natl. Acad. Sci. USA 91, 549–553.

Patel, P.H., Jacobo-Molina, A., Ding, J., Tantillo, C., Clark Jr., A.D., Raag, R., Nanni, R.G., Hughes, S.H., Arnold, E., 1995. Insights into DNA polymerization mechanisms from structure and function analysis of HIV-1 reverse transcriptase. Biochemistry 34, 5351–5363.

Ragno, R., Artico, M., De Martino, G., La Regina, G., Coluccia, A., Di Pasquali, A., Silvestri, R., 2005a. Docking and 3-D QSAR studies on indolyl aryl sulfones. Binding mode exploration at the HIV-1 reverse transcriptase non-nucleoside binding site and design of highly active *N*-(2-hydroxyethyl)carboxamide and *N*-(2-hydroxyethyl)carbohydrazide derivatives. J. Med. Chem. 48, 213–223.

Ragno, R., Frasca, S., Manetti, F., Brizzi, A., Massa, S., 2005b. HIV-reverse transcriptase inhibition: inclusion of ligand-induced fit by cross-docking studies. J. Med. Chem. 48, 200–212.

Ragno, R., Coluccia, A., La Regina, G., De Martino, G., Piscitelli, F., Lavecchia, A., Novellino, E., Bergamini, A., Ciaprini, C., Sinistro, A., Maga, G., Crespan, E., Artico, M., Silvestri, R., 2006. Design, molecular modeling, synthesis, and anti-HIV-1 activity of new indolyl aryl sulfones. Novel derivatives of the indole-2-carboxamide. J. Med. Chem. 49, 3172–3184.

Regina, G.L., Coluccia, A., Piscitelli, F., Bergamini, A., Sinistro, A., Cavazza, A., Maga, G., Samuele, A., Zanoli, S., Novellino, E., Artico, M., Silvestri, R., 2007. Indolyl aryl sulfones as HIV-1 non-nucleoside reverse transcriptase inhibitors: role of two halogen atoms at the indole ring in developing new analogues with improved antiviral activity. J. Med. Chem. 50, 5034–5038.

Schäfer, W., Friebe, W.G., Leinert, H., Mertens, A., Poll, T., von der Saal, W., Zilch, H., Nuber, B., Ziegler, M.L., 1993. Non-nucleoside inhibitors of HIV-1 reverse transcriptase: molecular modeling and X-ray structure investigations. J. Med. Chem. 36, 726–732.

Silvestri, R., Artico, M., 2005. Indolyl aryl sulfones (IASs): development of highly potent NNRTIs active against wt-HIV-1 and clinically relevant drug resistant mutants. Curr. Pharm. Des. 11, 3779–3806.

Silvestri, R., De Martino, G., La Regina, G., Artico, M., Massa, S., Vargiu, L., Mura, M., Loi, A.G., Marceddu, T., La Colla, P., 2003. Novel indolyl aryl sulfones active against HIV-1 carrying NNRTI resistance mutations: synthesis and SAR studies. J. Med. Chem. 46, 2482–2493.

Silvestri, R., Artico, M., De Martino, G., La Regina, G., Loddo, R., La Colla, M., Mura, M., La Colla, P., 2004. Simple, short peptide derivatives of a sulfonylindolecarboxamide (L-737,126) active in vitro against HIV-1 wild type and variants carrying non-nucleoside reverse transcriptase inhibitor resistance mutations. J. Med. Chem. 47, 3892–3896.

Sluis-Cremer, N., Arion, D., Parniak, M.A., 2000. Molecular mechanisms of HIV-1 resistance to nucleoside reverse transcriptase inhibitors (NRTIs). Cell. Mol. Life Sci. 57, 1408–1422.

Tomaras, G.D., Greenberg, M.L., 2001. Mechanisms for HIV-1 entry: current strategies to interfere with this step. Curr. Infect. Dis. Rep. 3, 93–99.